ISSN 1330-3651 (Print), ISSN 1848-6339 (Online)
Received: 21 June 2025; Accepted: 19 November 2025

https://doi.org/10.17559/TV-20250621002767
Original scientific paper

Influence of MIG Process Parameters Correction on Bead on Plate Welds Geometry

Milan MARÔNEK, Katarína BÁRTOVÁ, Jozef BÁRTA*

Abstract: This study investigates the influence of arc length correction and dynamic correction on the geometry and stability of bead-on-plate welds produced using the MIG Pulse Synergic process. S235 carbon steel was used as the base material, with Inconel 718 as the filler metal. Welds were evaluated through visual inspection, 3D scanning, and statistical analysis. Results showed that arc length correction had a significant impact on bead width, height, weld toe angle, and heat input, while dynamic correction had a more limited effect, primarily influencing process stability and bead width at extreme settings. The findings provide guidance for optimizing welding parameters to improve WAAM process.

Keywords: arc length correction (*ALC*); dynamic correction (*DC*); MIG; WAAM; weld bead geometry

1 INTRODUCTION

Additive manufacturing (AM) has transitioned from a prototyping curiosity to a strategic production technology for high-value metal components. Among the family of directed-energy deposition processes, Wire Arc Additive Manufacturing (WAAM) has emerged as the go-to route for fabricating large parts at high deposition rates compared to powder-based systems often at a fraction of the material and capital cost. While WAAM productivity is compelling, its industrial adoption still hinges on overcoming the metallurgical and geometric challenges that arise when building fully dense, structurally critical parts from demanding nickel superalloys.

Gas-Metal-Arc Welding (GMAW, or MIG) is the most productive technology in WAAM because the consumable wire is already the electrode, delivering deposition rates of 3-8 kg × h^{-1} an order of magnitude higher than laser/powder systems and equipment costs that are 70-80% lower than powder-bed machines. Compared with TIG-WAAM, GMAW offers approximately 2 times higher metal yield because of the constant wire feed, and spray/pulse variants generate a smoother bead with fewer lack-of-fusion defects.

Inconel 718 remains the aerospace standard for combustor casings, turbine discs, and rocket engine hardware thanks to its exceptional tensile strength (> 1050 MPa) and creep resistance up to 704 °C. Yet these advantages come with formidable welding challenges: segregation-driven Laves phase formation, solidification cracking in the interdendritic regions, and a steep thermal contraction gradient that can warp slender geometries.

Current research activities involve many topics; from parameter optimisation in relation to geometry of built-up component walls [1-6], through mapping the thermal fields and heat input on different material properties [7-9], microstructural changes in weld metal [7, 10-17], mechanical properties of WAAM produced components [10, 12, 17-21], heat treatment and its influence on improvement of material properties [10, 16, 17, 20] to residual stresses after the WAAM process [7, 22-24].

WAAM process parameters are crucial in terms of the occurrence of possible defects and costs associated with the machining of manufactured components. Manufacturers of welding power sources allow the operator to correct the set parameters to a certain extent, but they do not quantify the extent to which the welding parameters are corrected. This article focuses on the influence of arc length correction and dynamic correction of the Fronius TPS600i power source on the resulting geometric characteristics of bead on plate welds.

2 MATERIALS AND METHODS

S235 carbon steel, measuring 170 × 30 × 15 mm, was selected as the base material due to its cost-effectiveness. In additive manufacturing, the base is typically removed after the process, making a low-cost option preferable. The WAAM process is particularly economical for producing large, thin-walled components using high-cost alloys. For this reason, Inconel 718 alloy was used as the deposition material, supplied in the form of NiCro 718 MIG wire with a diameter of 1.2 mm. The filler wire's chemical composition wire based on the 3.1 inspection certificate delivered by the producer according to EN10204 is listed in Tab. 1.

Table 1 Chemical composition of NiCro 718 filer material / wt. %

C	Mn	Si	S	P	Cr	Ni	Mo
0.07	0.1	0.15	0.001	0.008	17.5	52	3
Al	Ti	Co	Cu	Nb + Ta	B	Fe	
0.4	0.9	0.05	0.05	5	0.005	Bal.	

Bead on plate welds (BPW) were produced in Pulse Synergic mode. The arc length correction (*ALC*) and dynamic correction (*DC*) were adjusted from the minimum to the maximum in three levels (−10, 0, 10), as permitted by the power source. During the arc length correction adjustments, the dynamic correction was set to the default value of 0, and vice versa, when adjusting the dynamic correction, the arc length correction was set to the default value of 0. Torch movement was carried out by First Welding Company Multiweld portal system. Torch movement length was 100 mm. HKS WeldAnalyst system with sampling frequency of 10 kHz was used to determine the RMS (root mean square) values of deposition current and voltage. High-purity argon (99.996%) was used as shielding gas at a flow rate of 17 l/min.

The geometry of the BPW was examined by GOM ATOS II TripleScan 3D optical scanner. For each BPW, ten virtual cross-sections were created to measure the width, height, and weld toe angle of the bead (Fig. 1, Fig. 2). The origin of virtual cross-sections was located 20 mm

from the weld bead start position. Particular virtual cross-sections were located 5 mm apart. The scanning data were analysed using the GraphPad Prism 8 statistical software. All data showed normal distribution. The ordinary one-way ANOVA was used for multiple comparisons. Used levels of significance were * $p \in$ <0.01; 0.05), ** $p \in$ <0.001; 0.01), **** $p <$ 0.0001. All error bars shown in figures represent standard deviation (SD).

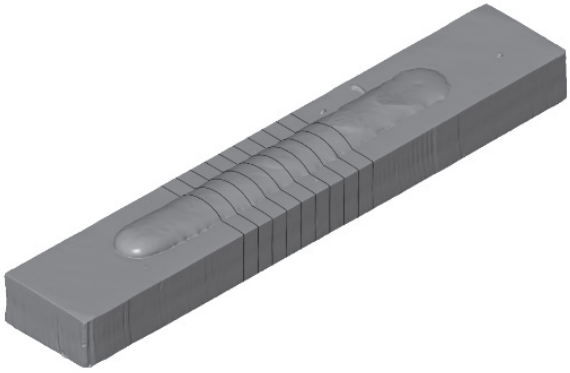

Figure 1 Virtual cross-sections positions

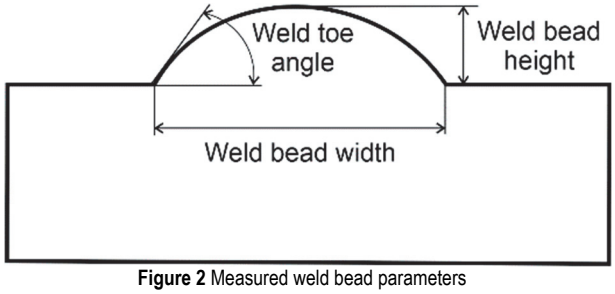

Figure 2 Measured weld bead parameters

3 RESULTS AND ACHIEVEMENTS

3.1 Visual Inspection

Visual inspection was realised according to ISO 17637 and did not reveal any imperfections. Fig. 3 to Fig. 8 show the appearance of particular BPW. As anticipated, increasing the arc length correction resulted in a wider BPW (Fig. 3, Fig. 5, Fig. 7). Similarly, the increase of arc length correction caused an increase in the fluctuations of the BPW width.

Figure 3 Bead appearance, *ALC* −10, *DC* 0

Figure 4 Bead appearance, *ALC* 0, *DC* −10

Figure 5 Bead appearance, *ALC* 0, *DC* 0

Figure 6 Bead appearance, *ALC* 0, *DC* 0

Figure 7 Bead appearance, *ALC* 10, *DC* 0

Figure 8 Bead appearance, *ALC* 0, *DC* 10

On the other hand, the change in the dynamic correction had almost no effect on the visual appearance of the BPW width (Fig. 4, Fig. 6, Fig. 8).

3.2 Welding Parameters Analysis

Tab. 2 presents the recorded process parameters along with the calculated heat input values. Tab. 2 shows that increasing the arc length correction not only increases the voltage but also the welding current, which in turn causes a significant increase in heat input (up to 91%). The increase in heat input is subsequently reflected in an increase in the BPW width, which is consistent with the findings of the visual inspection. Dynamic arc correction also had an effect on the specific heat input, but to a significantly lesser extent. Between the minimum and maximum of the dynamic correction, the heat input increased by only 16%.

Table 2 Parameters of welding regimes

Arc length correction	Dynamic correction	Process parameters				
		Current (RMS) / A	Voltage (RMS) / V	Heat input / J/mm	Deposition rate / mm/s	Wire feed rate / m/min
−10	0	228.7	13.9	636.6	5	8
0	0	240.1	16.7	803.3	5	8
10	0	290.5	20.9	1214.3	5	8
0	−10	234.6	15.9	745.0	5	8
0	10	237.7	18.1	862.0	5	8

Fig. 9 and Fig. 10 document the detailed course of the welding parameters for the individual settings of arc length correction and dynamic correction. Fig. 9 documents the change in the course of the parameters at different arc length corrections. As can be seen, despite the synergic pulse mode, periodically occurring short circuits were observed in the course of the welding parameters, which disappeared only when the arc length correction was set to maximum (Fig. 9).

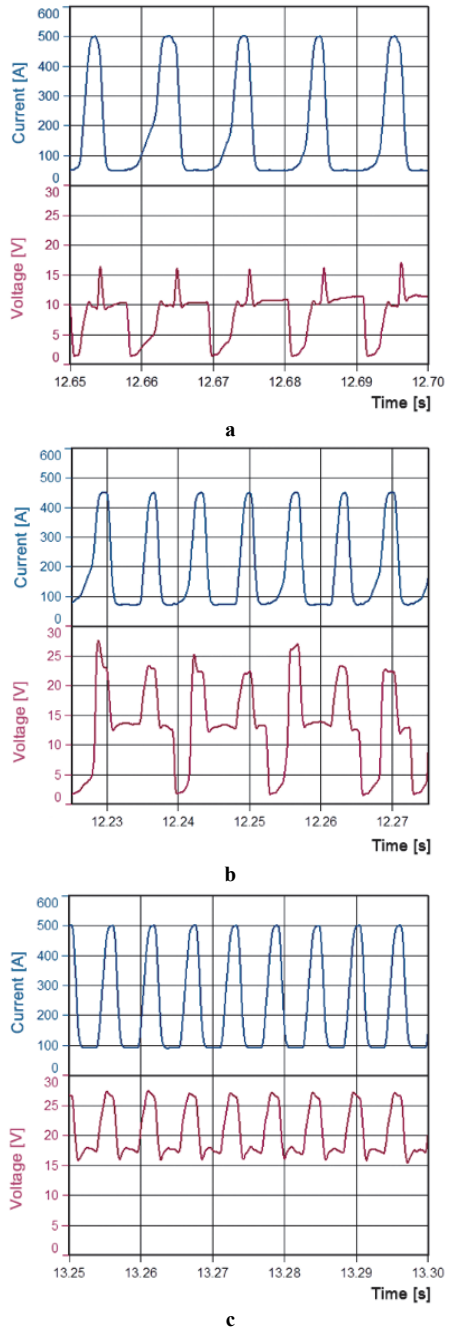

Figure 9 Recording of voltage and current waveforms, a - *ALC* −10, *DC* 0, b - *ALC* 0, *DC* 0, c - *ALC* 10, *DC* 0

On the other hand, voltage peaks for arc length corrections 0 and 10 reached approximately the same level. However, as expected, RMS voltage with increasing arc length correction raised. The voltage increase from arc length correction −10 to 0 was approximately 21%, the increase from arc length correction 0 to 10 was approximately 25%.

The change in the parameter curve during dynamic correction is shown in Fig. 10. The character of the short-circuit curve of the parameters does not change substantially when changing the dynamic correction from the value of −10 to 0 (Fig. 10a and Fig. 10b). The increase in RMS voltage in this case was only 5%. Increasing the dynamic correction to the value of 10 led to the disappearance of short circuits and stabilization of the process parameters (Fig. 10c).

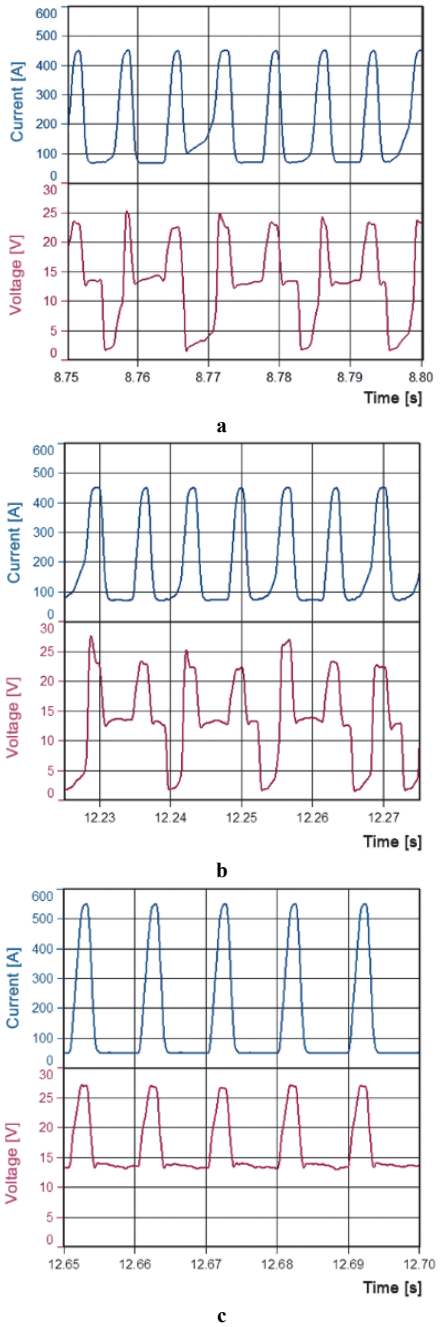

Figure 10 Recording of voltage and current waveforms, a - *ALC* 0, *DC* −10, b - *ALC* 0, *DC* 0, c - *ALC* 0, *DC* 10

3.3 Bead on Plate Weld Geometry Analysis

The average values of the width, height and angle of the BWP beads are given in Tab. 3.

Table 3 Evaluated weld bead geometries

Arc length correction	Dynamic correction	Bead geometry					
		Width / mm	St. dev. / mm	Height / mm	St. dev. / mm	Weld toe angle / °	St. dev. / °
−10	0	8.8	0.42	4.3	0.29	115	7.5
0	0	11.8	0.64	3.4	0.08	139	8.3
10	0	16.1	1.09	2.9	0.15	158	6.0
0	−10	11.5	0.12	3.6	0.17	138	3.6
0	10	12.2	0.26	3.5	0.08	143	4.0

ANOVA statistical analysis confirmed the extreme significance between the arc length correction in terms of width, height as well as weld toe angle of BPW (Fig. 11). Variance of BPW width (Fig. 11a) corresponds to the findings of visual inspection.

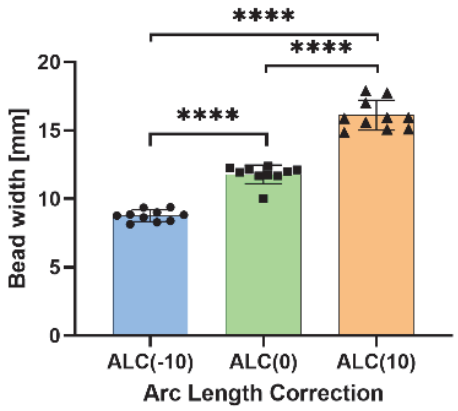

a

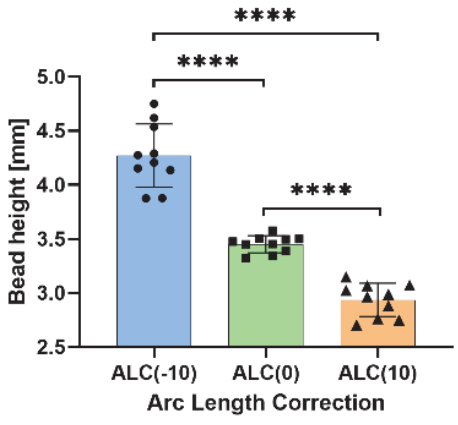

b

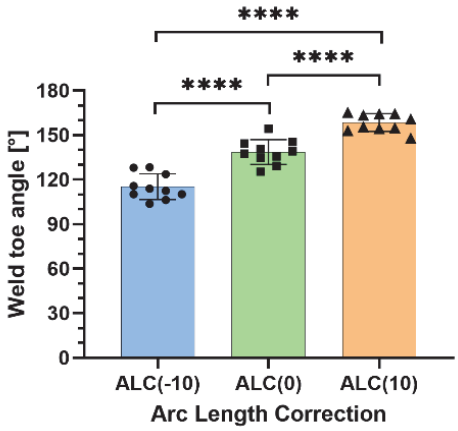

c

Figure 11 ANOVA of arc length correction, a - bead width, b - bead height, c - weld toe angle, **** $p < 0.0001$

From the point of view of the dynamic correction evaluation, statistical analysis confirmed significance in the case of bead width, but only between minimum and maximum correction (−10 and 10) (Fig. 12a). Regarding the bead height, statistical significance was confirmed only between dynamic correction −10 and 0 (Fig. 12b). In the case of weld toe angle, the evaluated data were not statistically significant at all (Fig. 12c).

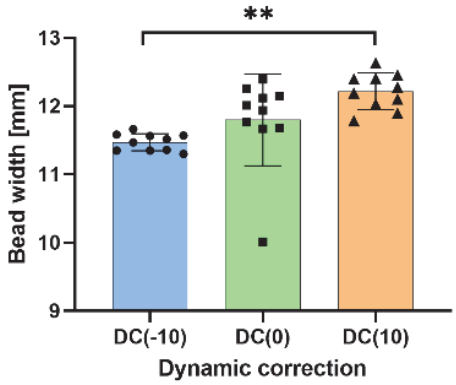

a

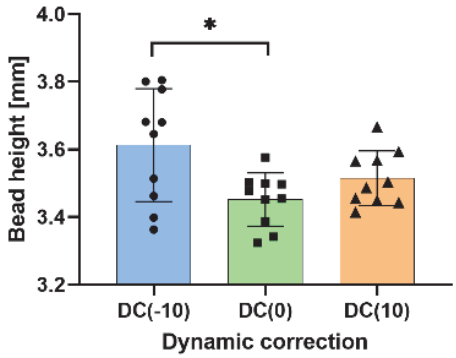

b

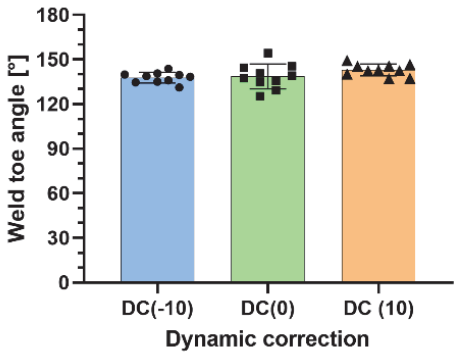

c

Figure 12 ANOVA of dynamic correction , a - bead width, b - bead height, c - weld toe angle, * $p \in$ <0.01; 0.05), ** $p \in$ <0.001; 0.01)

As previously mentioned, the arc length correction and dynamic correction affected the amount of heat input. Fig.

13 documents the effect of arc length correction and dynamic correction on the resulting heat input. As can be seen from Fig. 13, the effect of arc length correction on heat input is not linear and is higher compared to the effect of dynamic correction.

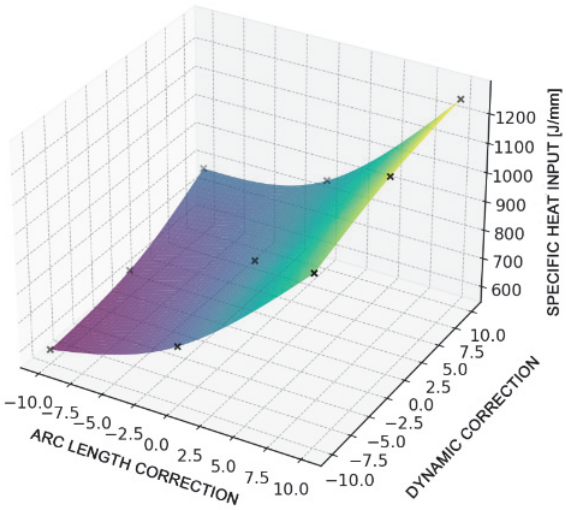

Figure 13 Influence of arc length correction and dynamic correction on specific heat input

These findings are consistent with established correlations between process parameters, heat input, and weld bead geometry reported in the literature. The observed trend of increasing bead width and decreasing reinforcement with rising heat input corresponds well with the results of Murugan and Parmar, who described similar relationships in gas metal arc surfacing processes [3]. Comparable conclusions were also drawn by Novelino et al. in studies of WAAM-CMT, where deposition parameters directly governed wall width and height, and by Tomków et al., who reported that small variations in arc parameters significantly affected bead shape in 316L GMAW [2, 4]. The non-linear increase in heat input with ALC and its geometric consequences also align with the findings of Cambon et al., who demonstrated that process parameters strongly influence weld pool morphology and the resulting residual stress distribution in WAAM structures [7]. Furthermore, the observed reduction in short-circuit frequency under high *ALC* and positive *DC* values agrees with reports by Terner et al. and Lee et al., who found that optimized pulse or synergic settings enhance arc stability and lead to more consistent bead geometries [5, 6].

4 CONCLUSIONS

The study evaluated the impact of arc length and dynamic corrections on MIG weld bead geometry. Based on the accomplished investigations, the following conclusions can be made:

- Arc length correction (*ALC*) has a significant effect on:
  - weld bead width, which increases with higher ALC.
  - weld bead height: Decreases as *ALC* increases.
  - weld toe angle becomes larger (flatter bead) with higher *ALC*.
  - heat input: Substantially increases with higher *ALC* (up to 91% increase).
  - process stability**: Higher *ALC* reduces short circuits, improving waveform smoothness.
- Dynamic correction (*DC*) influences the welding process less significantly, but:
  - causes slight increase in heat input (up to 16% from min to max),
  - significantly affects bead width only between extreme values ($DC = -10$ vs. $DC = 10$),
  - significantly affects bead height only between $DC = -10$ and 0,
  - has no statistically significant effect on the weld toe angle,
  - improves process stability at higher values (DC = 10), eliminating short circuits.
- Visual inspection and 3D scanning:
  - showed that *ALC* has a clear impact on bead geometry and appearance,
  - *DC* had minimal influence on visual appearance of the weld beads.
- Statistical analysis (ANOVA):
  - confirmed extreme significance (**** $p < 0.0001$) for *ALC* effects on all geometry parameters,
  - *DC* effects were significant only under certain comparisons.

Acknowledgement

This work was supported by the Slovak Research and Development Agency under the contract No. APVV-20-0259.

5 REFERENCES

[1] Senthilkumar, B., Kannan, T., & Surendran, P. (2015). Influence of welding process parameters on bead geometry - A review. *Journal of Mechanical and Mechanics Engineering*, *1*(3).

[2] Novelino, A. L. B., Carvalho, G. C., & Ziberov, M. (2022). Influence of WAAM-CMT deposition parameters on wall geometry. *Advances in Industrial and Manufacturing Engineering*, *5*, 100105. https://doi.org/10.1016/j.aime.2022.100105

[3] Murugan, N. & Parmar, R. S. (1994). Effects of MIG process parameters on the geometry of the bead in the automatic surfacing of stainless steel. *Journal of Materials Processing Technology*, *41*, 381-398. https://doi.org/10.1016/0924-0136(94)90003-5

[4] Tomków, J. et al. (2023). Impact of gas metal arc welding parameters on bead geometry and material distortion of AISI 316L. *Journal of Manufacturing and Materials Processing*, *7*(4), 123. https://doi.org/10.3390/jmmp7040123

[5] Lee, H. K., Kim, J., Pyo, C., & Kim, J. (2020). Evaluation of bead geometry for aluminum parts fabricated using additive manufacturing-based wire-arc welding. *Processes*, *8*(10), 1211. https://doi.org/10.3390/pr8101211

[6] Terner, M., Bayarsaikhan, T. A., Hong, H. U., & Lee, J. H. (2017). Influence of gas metal arc welding parameters on the bead properties in automatic cladding. *Journal of Welding and Joining*, *35*(1), 16-25. https://doi.org/10.5781/JWJ.2017.35.1.16

[7] Cambon, C., Bendaoud, I., Rouquette, S., & Soulié, F. (2022). A WAAM bench mark: From process parameters to thermal effects on weld pool shape, microstructure and

residual stresses. *Materials Today Communications*, *33*, 104235. https://doi.org/10.1016/j.mtcomm.2022.104235

[8] Chamim, M., Widodo, T. D., Purnowidodo, A., & Darmadi, D. B. (2025). Impact of welding thermal cycle on corrosion rate in the bottom area of AISI 308 L deposits fabricated by WAAM-GTAW. *Journal of Alloys and Metallurgical Systems*, *11*, 100196. https://doi.org/10.1016/j.jalmes.2025.100196

[9] Chamim, M., Darmadi, D. B., Purnowidodo, A., Widodo, T. D., & Ismail, Z. (2024). Influence of the welding thermal cycle on δ-ferrite evolution in the first layer of austenitic stainless steel (ASS) 308L produced by WAAM-GTAW. *Case Studies in Thermal Engineering*, *64*, 105489. https://doi.org/10.1016/j.csite.2024.105489

[10] Luna, V. et al. (2022). Comprehensive and comparative heat treatment of additively manufactured Inconel 625 alloy and corresponding microstructures and mechanical properties. *Journal of Manufacturing and Materials Processing*, *6*(5). https://doi.org/10.3390/jmmp6050107

[11 Asala, G., Khan, A. K., Andersson, J., & Ojo, O. A. (2017). Microstructural analyses of ATI 718Plus® produced by wire-arc additive manufacturing process. *Metallurgical and Materials Transactions A*, *48*(9), 4211-4228. https://doi.org/10.1007/s11661-017-4162-2

[12] Solomon, I. J., Srinivas, J., Leon, S. J., Ramesh, A., Rohith, I. J., & Senthil, T. S. (2024). Mechanical and microstructural investigation of multi-layered Inconel 825 wall fabricated using CMT-based WAAM. *Journal of Alloys and Metallurgical Systems*, *8*, 100115. https://doi.org/10.1016/j.jalmes.2024.100115

[13] Revilla, R. I. et al. (2020). Microstructure and corrosion behavior of 316L stainless steel prepared using different additive manufacturing methods: A comparative study bringing insights into the impact of microstructure on their passivity. *Corrosion Science*, *176*, 108914. https://doi.org/10.1016/j.corsci.2020.108914

[14] Le, V. T. & Mai, D. S. (2020). Microstructural and mechanical characteristics of 308L stainless steel manufactured by gas metal arc welding-based additive manufacturing. *Materials Letters*, *271*, 127791. https://doi.org/10.1016/j.matlet.2020.127791

[15] Clark, D., Bache, M. R., & Whittaker, M. T. (2010). Microstructural characterization of a polycrystalline nickel-based superalloy processed via tungsten-inert-gas-shaped metal deposition. *Metallurgical and Materials Transactions B*, *41*(6), 1346-1353. https://doi.org/10.1007/s11663-010-9410-4

[16] Velmurugan, S., Babu, N., & Santhosh, V. (2025). Effect of post-heat treatment on corrosion resistance and microstructural characteristics of CMT-WAAM Inconel 718 in 3.5% NaCl solution. *Journal of the Indian Chemical Society*, *102*(4), 101625. https://doi.org/10.1016/j.jics.2025.101625

[17] Chen, Z. & Soh, G. S. (2022). Microstructure and mechanical properties of wire arc additive manufactured (WAAM) Inconel 718 parts via post heat treatments. *Materials Today: Proceedings*, *70*, 567-573. https://doi.org/10.1016/j.matpr.2022.09.592

[18] Vora, J., Parmar, H., Chaudhari, R., Khanna, S., Doshi, M., & Patel, V. (2022). Experimental investigations on mechanical properties of multi-layered structure fabricated by GMAW-based WAAM of SS316L. *Journal of Materials Research and Technology*, *20*, 2748-2757. https://doi.org/10.1016/j.jmrt.2022.08.074

[19] Wang, J. et al. (2024). Weakening the mechanical property anisotropy of additively manufactured medium entropy alloy by controlling the cellular structure. *Additive Manufacturing*, *89*, 104303. https://doi.org/10.1016/j.addma.2024.104303

[20] Vishnukumar, M., Muthupandi, V., & Jerome, S. (2022). Effect of post-heat treatment on the mechanical and corrosion behaviour of SS316L fabricated by wire arc additive manufacturing. *Materials Letters*, *307*, 131015. https://doi.org/10.1016/j.matlet.2021.131015

[21] Le, V. T., Mai, D. S., Doan, T. K., & Paris, H. (2021). Wire and arc additive manufacturing of 308L stainless steel components: Optimization of processing parameters and material properties. *Engineering Science and Technology, an International Journal*, *24*(4), 1015-1026. https://doi.org/10.1016/j.jestch.2021.01.009

[22] Sun, J., Hensel, J., Köhler, M., & Dilger, K. (2021). Residual stress in wire and arc additively manufactured aluminum components. *Journal of Manufacturing Processes*, *65*, 97-111. https://doi.org/10.1016/j.jmapro.2021.02.021

[23] Abusalma, H., Eisazadeh, H., Hejripour, F., Bunn, J., & Aidun, D. K. (2022). Parametric study of residual stress formation in wire and arc additive manufacturing. *Journal of Manufacturing Processes*, *75*, 863-876. https://doi.org/10.1016/j.jmapro.2022.01.043

[24] Wu, Q., Mukherjee, T., De, A., & DebRoy, T. (2020). Residual stresses in wire-arc additive manufacturing: Hierarchy of influential variables. *Additive Manufacturing*, *35*, 101355. https://doi.org/10.1016/j.addma.2020.101355

Contact information:

Milan MARÔNEK
Slovak University of Technology in Bratislava,
Faculty of Materials Science and Technology in Trnava,
Institute of Production Technologies,
Paulínska 16, 91701 Trnava, Slovakia
E-mail: milan.maronek@stuba.sk

Katarína BÁRTOVÁ
Slovak University of Technology in Bratislava,
Faculty of Materials Science and Technology in Trnava,
Institute of Production Technologies,
Paulínska 16, 91701 Trnava, Slovakia
E-mail: jozef.barta@stuba.sk

Jozef BÁRTA
(Corresponding author)
Slovak University of Technology in Bratislava,
Faculty of Materials Science and Technology in Trnava,
Institute of Production Technologies,
Paulínska 16, 91701 Trnava, Slovakia
E-mail: jozef.barta@stuba.sk